

# The chronic cerebral hypoperfusion model induces proinflammatory cascades in Alzheimer's disease

Zahra Abedi<sup>1</sup>, Hamidon Basri<sup>1\*</sup>, Zurina Hassan<sup>2\*</sup>, Liyana Najwa Inche Mat<sup>1</sup>, Huzwah Khaza'ai<sup>1</sup> and Razana Binti Mohd Ali<sup>1</sup>

<sup>1</sup> Faculty of Medicine and Health Sciences, Universiti Putra Malaysia, Selangor, Malaysia.

<sup>2</sup> Centre for Drug Research, Universiti Sains Malaysia, Penang, Malaysia.

\* Correspondence: [hamidon@upm.edu.my](mailto:hamidon@upm.edu.my), [zurina\\_hassan@usm.my](mailto:zurina_hassan@usm.my); Tel.: +603-97692570, +604-6532726

**Received:** 1 December 2023; **Accepted:** 31 March 2024; **Published:** 19 May 2024

**Edited by:** Pike See Cheah (Universiti Putra Malaysia, Malaysia)

**Reviewed by:** Siti Rafidah Yusof (Universiti Sains Malaysia, Malaysia); Seong Lin Teoh (Universiti Kebangsaan Malaysia, Malaysia)

<https://doi.org/10.31117/neuroscirn.v7i2.315>

**Abstract:** Cerebral neuroinflammation has emerged as a significant pathway contributing to the progression of Alzheimer's disease (AD) pathology. Research implicates the NOD-like receptor family, pyrin domain containing 3 (NLRP3) inflammasome complex, initiating caspase 1-mediated maturation of interleukin-1  $\beta$  (IL-1 $\beta$ ) and interleukin-18 (IL-18). This study investigates whether chronic cerebral hypoperfusion (CCH), induced via permanent bilateral occlusion of the common carotid arteries (PBOCCA), leads to cognitive dysfunction and NLRP3 inflammasome activation. Twenty male Sprague Dawley (SD) rats underwent PBOCCA to induce CCH. Two weeks post-surgery, locomotor and Morris water maze (MWM) tests were conducted to examine motor functions, spatial learning, and memory, respectively. The gene expression levels of cathepsin B, NLRP3, an apoptosis-associated speck-like protein containing a caspase recruitment domain (ASC), and caspase-1 were analysed using real-time PCR, while the expression levels of the inflammatory cytokines were estimated using the ELISA method. Structural damage to the hippocampus was assessed using hematoxylin and eosin (HE) staining. Escape latencies and time spent in specific quadrants in PBOCCA significantly increased compared to sham-operated animals. There was no notable difference in locomotor activity between the PBOCCA and sham-operated groups. The number of pyknotic neurons with cytoplasmic shrinkage increased in the hippocampus. Gene expression of cathepsin B, NLRP3, ASC, and caspase-1 was upregulated in the PBOCCA group. The expression levels of IL-1 $\beta$ , IL-18, interleukin-6 (IL-6), and amyloid- $\beta$  1-42 (A $\beta$  1-42) were elevated in the PBOCCA group relative to sham. The findings confirm NLRP3 inflammasome induction, cognitive dysfunction, and inflammatory cytokines associated with AD and cerebral ischemia. The PBOCCA model provides a valuable tool for studying neurodegenerative including AD.

**Keywords:** Chronic cerebral hypoperfusion, PBOCCA, Alzheimer's disease, Neuroinflammation, Inflammasome, Learning and memory

©2024 by **Abedi et al.** for use and distribution according to the Creative Commons Attribution (CC BY-NC 4.0) license (<https://creativecommons.org/licenses/by-nc/4.0/>), which permits unrestricted non-commercial use, distribution, and reproduction in any medium, provided the original author and source are credited.

## 1.0 INTRODUCTION

CCH is frequently observed due to different cerebral vascular disorders and hemodynamic and blood alterations ([Scheffer et al., 2021](#)). Recent investigations have highlighted the significant involvement of CCH in neurodegeneration and dementia, encompassing both vascular dementia (VaD) and AD ([Rajeev et al., 2022](#); [Scheffer et al., 2021](#)). CCH contributes to neurodegeneration and the development of AD through diverse mechanisms, such as the induction of oxidative stress, accumulation, and exacerbation of A $\beta$ , hyperphosphorylation of tau protein, impairment of synaptic function, neuronal loss, white matter lesions, and neuroinflammation ([Chen et al., 2022](#)).

AD, the second most common type of dementia, is linked to cerebral hypoperfusion, which may contribute to cognitive impairment ([Bhuvanendran et al., 2019](#)). One of the main AD pathogenic characteristics is neuroinflammation, which is primarily associated with the deposition of cerebral A $\beta$  accumulation, neurofibrillary tangles resulting from the loss of neurons and microtubule-associated proteins phosphorylation ([Španić et al., 2022](#)). These changes are closely related to innate immune system impairment in the brain, whereby there is an inflammatory immune response of glial cells and nonspecific injury to brain blood vessels, leading to the overactivation of inflammasomes ([Hardy & Selkoe, 2002](#); [Mathys et al., 2019a, 2019b](#)).

Inflammasome overactivation is a major feature of neuroinflammation in AD. The NLRP3 inflammasome, which comprises NLRP3, an apoptosis-associated speck-like protein containing a caspase recruitment domain (ASC) and pro-caspase-1, can trigger caspase-1 activation, leading to the initiation of pyroptosis and the subsequent processing and release of IL-1  $\beta$  and IL-18 ([Li et al., 2022](#); [Zhao et al., 2023](#)). Under normal physiological conditions, the NLRP3 inflammasome, integral to the innate immune response, orchestrates host defence by recognising pathogen-associated or danger-associated signals. Physiologically, it regulates pro-inflammatory cytokine release, including IL-1 $\beta$  and IL-18, promoting immune response, pyroptosis, and tissue repair. However, dysregulated NLRP3 activation can lead to pathological inflammation, implicating its intricate role in immune homeostasis and disease pathogenesis ([Abaricia et al., 2021](#)).

Therefore, understanding the balance in NLRP3 inflammasome activation is crucial for normal immune function and preventing pathological conditions. The NLRP3 inflammasome can be triggered by various

stimuli, such as disruptions in Ca<sup>2+</sup> signalling, efflux of K<sup>+</sup>, production of reactive oxygen species (ROS), impairment of mitochondrial function, and rupture of lysosomes. Recently, researchers have highlighted the significant role of autophagy in regulating the NLRP3 inflammasome in inflammatory nervous system disorders ([Zhao et al., 2021](#)). However, the related mechanisms are not entirely clarified. Investigating the relationship between CCH, NLRP3 inflammasome activation, and cognitive dysfunction is crucial for advancing our understanding of AD pathophysiology ([Poh et al., 2022](#)). CCH induces sustained cerebral blood flow reduction, triggering neuroinflammatory responses. The NLRP3 inflammasome, a key mediator, produces proinflammatory cytokines ([Xu et al., 2023](#)).

Examining the intricate connections between CCH, inflammasome activation, and cognitive decline elucidates potential mechanistic links in AD progression, offering valuable insights for targeted therapeutic strategies. Numerous animal models of CCH have been generated in rodents by inducing cerebral blood flow (CBF) restriction. These models serve the purpose of studying the contributions and underlying mechanisms of CCH in cognitive decline while also assessing the effectiveness of potential medications for therapeutic intervention ([Yu et al., 2022](#)). The rat model most frequently employed involves permanent bilateral common carotid arteries occlusion, also known as 2-vessel occlusion (PBOCCA /2-VO) ([Lee et al., 2021](#); [Xu et al., 2020](#); [Yu et al., 2022](#)).

Multiple research investigations have documented spatial memory impairments in this CCH model ([Hazalin et al., 2020](#); [Lin et al., 2023](#)). After occlusion surgery, various pathological changes occur in the hippocampus, including decreased levels of postsynaptic density protein 95 and synaptophysin, accumulation of oligomeric A $\beta$  over time, central cholinergic dysfunction, and increased oxidative damage ([Ahad et al., 2023](#); [Kumaran et al., 2022](#); [Roy et al., 2022](#); [Wang et al., 2010](#)). Additionally, there is evidence of white matter damage, elevated pro-inflammatory cytokines such as IL-1 $\beta$  and IL-6, decreased anti-inflammatory cytokines like IL-4 and IL-10, disruption of lysosomal function, and abnormal autophagy with accumulation of autolysosomes ([Calabrese et al., 2018](#); [Simats & Liesz, 2022](#); [Su et al., 2017](#); [Su et al., 2018](#); [Zhao et al., 2021](#)).

Since previous research revealed the role of autophagy in the regulation of the NLRP3 inflammasome, disruption of lysosomal function and abnormal autophagy through CCH, this study aims to investigate

the hypothesis that CCH induced by the PBOCCA leads to cognitive dysfunction, activation of NLRP3 inflammasomes, as well as alterations in cathepsin B levels in both the hippocampus and frontal cortex. The selection of the hippocampus and frontal cortex stems from their central roles in neuroinflammation linked to NLRP3 inflammasome activation and AD. The hippocampus, vital for cognition, and the frontal cortex, governing executive functions, offer insight into inflammasome-related neurodegeneration ([Cheon et al., 2020](#)). Examining inflammasome markers in these regions enhances understanding of Alzheimer's pathology.

## 2.0 MATERIALS AND METHODS

### 2.1 Animals

The Animal Research and Service Centre (ARASC), Universiti Sains Malaysia (USM) provided a total of 20 male Sprague Dawley (SD) rats weighing between 250g and 300 g for this study. The rats were housed in a controlled environment, with a 12:12 light/dark cycle and unrestricted access to food and water. The temperature was maintained at  $24^{\circ}\text{C} \pm 1^{\circ}\text{C}$ , and the humidity was controlled at 60%. The Animal Ethics Committee Universiti Sains Malaysia reviewed and approved all experimental procedures involving animals under reference number USM/IACUC/2019/(119)/(1002).

### 2.2 Surgery and experimental design

The rats were allocated randomly to perform permanent bilateral common carotid artery occlusion (PBOCCA) and sham surgery as described previously ([Damodaran et al., 2014](#); [Pappas et al., 1996](#); [Wang et al., 2018](#)). Anesthesia was administered intraperitoneally using a mixture of ketamine and xylazine (80 mg/kg and 10 mg/kg). In the PBOCCA group, the carotid arteries were exposed through a ventral midline incision, separate from their sheaths and vagus nerves, and ligated with a 4–0 monofilament nylon suture approximately around 8–10 mm below the external carotid artery origin. The incision was then sutured, and the rats were kept at  $25^{\circ}\text{C}$ . The exact surgical procedure was performed in the sham group, but no arteries were tied. The survival rate was 16/20 rats, assigned randomly to two groups, with 8 per group. After two weeks, the rats were subjected to behavioural tasks. At the end of behavioural tasks, on day 22, the animals from each group were sacrificed using  $\text{CO}_2$ , and the brains were procured for RT-PCR, ELISA, and histochemical staining analyses.

### 2.3 Morris water maze task

Two weeks after surgery, the MWM was conducted with slight modifications to a previously described protocol ([Vorhees & Williams, 2006](#)). One day before training, all rats underwent a pre-training session in which they were given free access to a pool with a depth of 70 cm and a diameter of 160 cm for 60 seconds without an escape platform. During the formal training, the pool was filled with water maintained at  $25 \pm 1^{\circ}\text{C}$  and divided into four quadrants with a 10 cm diameter hidden platform situated 2 cm below the water surface to make it invisible in the central part of the west, south quadrant. This quadrant was designated as the target quadrant, and the platform's position remained constant throughout the experiment. The training for finding the hidden platform was conducted on four consecutive days with eight daily trials. The rats underwent four trials each time, followed by a rest period, before proceeding to the next four trials. This cycle was repeated for a total of eight trials per day, with four separate trials conducted each time.

The rat was released into the pool from different starting points on each training trial, and the starting point varied each day. Once the rat located the hidden platform, it was permitted to remain on it for 15 seconds. The time taken for the rat to reach the hidden platform (escape latency) was measured using a stopwatch and recorded via camera for each trial session. There was a two-minute interval between each trial. If the rat failed to locate the platform within 60 seconds, it was gently guided to the platform and allowed to stay on it for 15 seconds, with these instances being recorded as a score of 60 seconds.

On the 5th day, each rat completed a 60 s probe trial to assess the rats' spatial memory. The platform was taken away, and a probe trial performance was carried out, in which each rat was allowed to swim freely for 60 seconds. The duration of each rat spent on the target quadrant was recorded and analysed using a smart video tracking system (Harvard Apparatus, USA). The percentage of crossing in the target quadrant where the former platform was previously located represented the ratio between the time spent crossing that quadrant and the total time spent crossing all the quadrants, calculated as a measure of spatial reference memory.

### 2.4 Locomotor activity

The locomotor activity of both groups was evaluated using the automated open-field apparatus (Pan Lab, Spain) two weeks after the surgery. This apparatus had a Perspex cage (height: 40 cm; length: 90 cm; width: 90

cm), with the bottom partitioned into five zones. The detection unit was composed of a 45 × 45 cm frame that contained 16 × 16 infrared beams at an interval of 2.5 cm on the side, yielding 32 cells in one frame. An offline tracking and analysis were done on the rat's movements. Each rat was placed in the middle of an open field for 20 minutes with 8 rats per group, and the spontaneous activity (ambulation and rearing) was monitored and recorded.

## 2.5 Hematoxylin and eosin (HE) staining

The histochemical staining was performed as per established procedures (Damodaran et al., 2014). Initially, the animals were given an intraperitoneal overdose of pentobarbital (100 mg/kg) to anaesthetise them. Next, normal saline was used for trans-cardiac perfusion to achieve pre-fixation. The brain was paraffin-embedded and sliced into 4-µm-thick coronal sections. Since the cholinergic projection starts from the frontal cortex to the hippocampus, therefore the sections corresponding to the Cornu Ammonis 1 (CA1) of the hippocampus were deparaffinised, rehydrated, stained, and examined at x400 magnification using an Olympus-BX53 microscope by an investigator blinded to the treatment history. Then, the features of neuronal death were checked (counting the numbers of pyknotic neurons with cytoplasmic shrinkage) in CA1 for both Sham and PBOCCA groups. Then, we analyse it with one-way ANOVA with Bonferroni's post hoc tests and report it as H&E indices.

## 2.6 Reverse transcription and quantitative real-time PCR

According to the manufacturer's protocol, total RNA was isolated from hippocampus and frontal cortex tissue using Monarch Total RNA Miniprep kit (New England Biolabs, USA). Subsequently, 1µg of RNA per sample was reverse transcribed to synthesise single-strand cDNA using LunaScript® RT SuperMix Kit (New England Biolabs, USA) according to the protocol provided by the manufacturer. While the genomic DNA elimination reaction was incubated for 2 minutes at 45°C, the reverse transcription reaction cycle conditions were incubated at 25°C, 55°C, and 95°C for 2,10, and 1 minute, respectively.

mRNA expressions of NLRP3, ASC, Caspase-1, and cathepsin B were analysed. The expression of Glyceraldehyde 3-phosphate dehydrogenase (GAPDH) was used to normalise the expression levels of the cytokines. The primers were reconstituted to prepare

100 µM stock solutions. The RT-PCR was conducted according to Luna Universal qPCR Master Mix kit (New England Biolabs, USA) protocol provided by the manufacturer at MiniOpticon™ Real-Time Detection System (Bio-Rad). The RT-PCR master mix, consisting of 10 µl master mix, 0.5 µl each of forward and reverse primers, 2 µl cDNA, and 7 µl Nuclease-free Water, in a total volume of 20 µL, was used for quantification of both target and reference genes. Cycling conditions for RT-PCR included enzyme activation (95 °C for 60 s), 40 cycles of denaturation (95 °C for 15 s), annealing or extension (60 °C for 30 s), and melt curve analysis at 65–95 °C for 5 s. Primers referenced in **Table 1** were provided by Integrated DNA Technologies (IDT).

**Table 1.** Primers for real-time PCR

Gene	Forward (5'-3')	Reverse (5'-3')
<b>NLRP3</b>	CCAGGGCTCTGTTC ATTG	CCTTGGCTTTCACCT CG
<b>ASC</b>	CCCATAGACCTCAC TGATAAAC	AGAGCATCCAGCAA ACCA
<b>Caspase-1</b>	AGGAGGGAATATG TGGG	AACCTTGGGCTTGT CTT
<b>Cathepsin B</b>	GTTGGGTTTCAGCGA GGACATA	GCGATGGTCGGGCA ATT
<b>GAPDH</b>	CAGCCTCGTCTCAT AGACAAGATG	AAGGCAGCCCTGGT AACCA

## 2.7 Enzyme-linked immunosorbent assay (ELISA) analysis

ELISA was used to determine IL-1β, IL-18, IL-6 and Aβ1-42 levels in the hippocampus and frontal cortex samples isolated from the Sham and PBOCCA brain. Commercially available ELISA kits (Elabscience, MD, USA) for rat IL-1β (E-EL-R0012), IL-18 (E-EL-R0567) and IL-6 (E-EL-R0015) and Aβ1-42 (E-EL-R1402) were performed according to the manufacturer's instructions. Absorbance measurements were carried out by a microplate spectrophotometer (Thermofisher Automated ELISA Reader).

## 2.8 Statistical analysis

The findings are presented as the mean ± standard error of the mean (SEM). Statistical analysis for MWM, probe trial, and locomotor activity was performed using an unpaired Student's t-test. Other group means were compared by one-way ANOVA with Bonferroni's post hoc tests. A p<0.05 was considered statistically significant. Statistical analysis was performed using Graph Pad Prism (version 8).

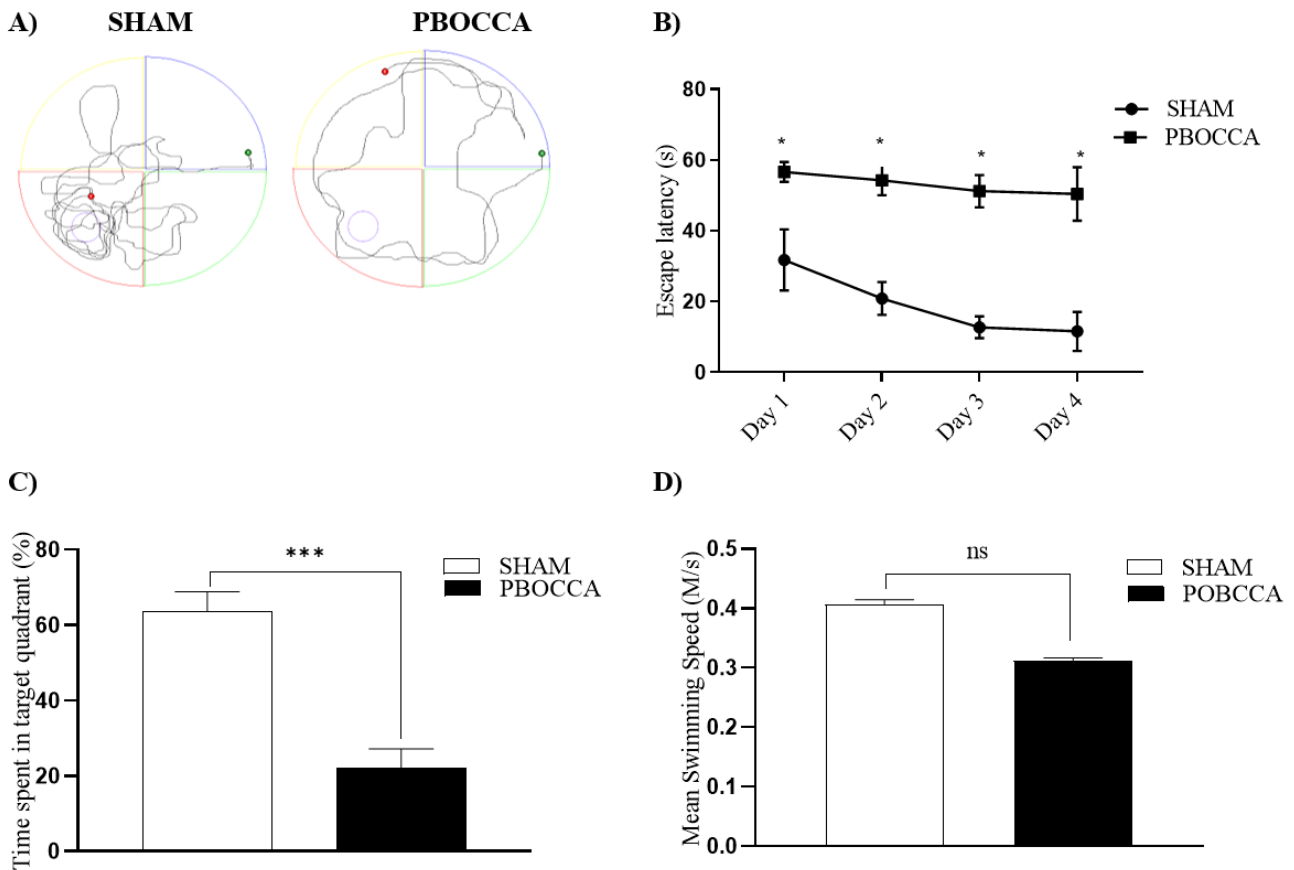


**Figure 1.** The CCH-induced spatial learning and memory deficits based on the Morris water maze analysis. **(A)** Typical swim paths. **(B)** Escape latency. **(C)** Time spent in the target quadrant. **(D)** The mean swimming speeds. Data are expressed as mean  $\pm$  SEM. (n = 8 rats/group, p < 0.05 Sham vs. PBOCCA).

### 3.0 RESULTS

#### 3.1 PBOCCA induced cognitive deficits.

The MWM is conducted to assess the spatial learning and memory of PBOCCA and sham-operated rats, as shown in **Figure 1**. The typical swimming paths of rats in each group were recorded during the training trial, as shown in **Figure 1A**, and their mean of escape latency was measured over four days.

Our study revealed that the mean escape latency between the PBOCCA and sham groups was significantly different with p = 0.01 (Day 1), p = 0.002 (Day 2), p = 0.007 (Day 3) and p = 0.004 (Day 4) where the PBOCCA groups exhibited higher escape latencies, implying slower spatial learning compared to the sham group, as shown in **Figure 1B**. On the fifth day, the platform was taken away, and a probe trial performance was carried out whereby each rat was allowed to swim freely for 60 seconds. The duration of each rat spent in the target quadrant was observed and recorded. Results from probe trial performance showed that the PBOCCA group spent significantly less time in the target quadrant than the Sham group, indicating decreased spatial memory

(p = 0.008), as shown in **Figure 1C**. The rats' movement was analysed using the SMART software system, and there were no significant differences in swimming speed between the PBOCCA and Sham-operated groups (**Figure 1D**, p = 0.6).

#### 3.2 PBOCCA did not impair motor performance.

The locomotor activity of rats in both PBOCCA and Sham-operated groups was evaluated using a 20-minute open-field test session, and the results are presented in **Figure 2**. There was no significant difference in the locomotor activities, total distance travel, and mean velocity recorded between the two groups (**Figure 2A**, p = 0.3961; **Figure 2B**, p = 0.2994; **Figure 2C**, p = 0.3721). This finding indicates that the PBOCCA did not impair the motor performance of the rat, and both groups showed similar levels of activity and mobility during the test.

#### 3.3 PBOCCA-induced hippocampal neuronal damage

The histological analysis using HE stains of hippocampal pyramidal neurons revealed a notable difference between the PBOCCA and Sham-operated groups. In the

Sham group, the pyramidal neuron was observed to be properly aligned along the striatum pyramidal, and the individual neurons exhibited clear nucleoli and abundant cytoplasm, as shown in **Figure 3A**. In contrast, in the PBOCCA groups, the HE-stained section showed disrupted cellular arrangement in hippocampal CA1 and significantly increased pyknotic neuron numbers with cytoplasmic shrinkage. The HE index was significantly different among groups (**Figure 3B**,  $p < 0.001$ ), with the PBOCCA displaying the highest value ( $p < 0.05$  compared to the Sham control group).

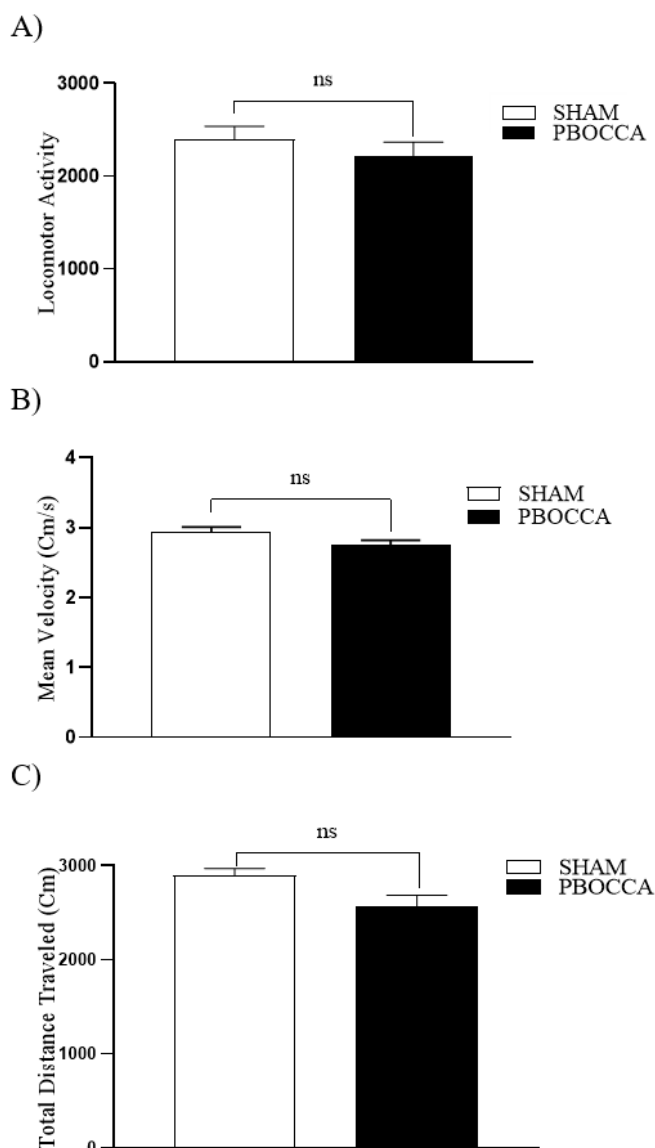


**Figure 2.** (A) Locomotor activity, (B) mean velocity and (C) total distance travelled in an open field apparatus of PBOCCA and sham-operated rats 2 weeks after the surgery. Data are expressed as mean  $\pm$  SEM. (n=8 rats/group sham vs. PBOCCA).

### 3.4 PBOCCA incited the gene expression

Since disruption of lysosomal membranes and cathepsin B release are required for NLRP3 inflammasome activation, we measured the levels of cathepsin B mRNA expression in the CCH-induced hippocampus and frontal cortex by real-time PCR (**Figure 4**). The mRNA expression levels of NLRP3, caspase-1, ASC and cathepsin B in PBOCCA rats were significantly increased compared to Sham control groups in the hippocampus region (**Figure 4A**;  $p = 0.0057$ , **Figure 4B**;  $p = 0.0010$ , **Figure 4C**;  $p = 0.0015$ , **Figure 4D**;  $p = 0.0061$ ). In the frontal cortex region, all levels of gene expression showed a significant upregulation in PBOCCA groups compared to the Sham group (**Figure 4A**;  $p = 0.0091$ , **Figure 4B**;  $p = 0.0070$ , **Figure 4C**;  $p = 0.0021$ , **Figure 4D**;  $p = 0.0055$ ).

### 3.5 PBOCCA activated inflammatory response

Astrocyte and neuron activation status is closely linked to the local neuroinflammatory state. Excessive caspase-1 levels can trigger IL-1 $\beta$  and IL-18. Therefore, we measured the levels of IL-1 $\beta$ , IL-18 and IL-6 as proinflammatory cytokines and A $\beta$ 1-42 in the hippocampus and frontal cortex by ELISA (**Figure 5**). The expression level of these proteins in PBOCCA rats was significantly increased in the hippocampus area compared to Sham groups (**Figure 5A**;  $p = 0.0099$ ; **Figure 5B**;  $p = 0.0297$ ; **Figure 5C**;  $p = 0.0041$ ; **Figure 5D**;  $p = 0.0416$ ). In PBOCCA rats, the levels of IL-1 $\beta$ , IL-18, IL-6 and A $\beta$ 1-42 were significantly elevated compared to the Sham group in the frontal cortex region (**Figure 5A**;  $p = 0.0211$ ; **Figure 5B**;  $p = 0.0111$ ; **Figure 5C**;  $p = 0.0153$ ; **Figure 5D**;  $p = 0.0191$ ).

## 4.0 DISCUSSION

CCH is considered a contributing factor to both VaD ([Zhao et al., 2014](#)) and AD ([Park et al., 2019](#)). However, the precise mechanisms by which CCH leads to cognitive impairment and contributes to the development of Alzheimer's pathology remain insufficiently understood. In our study, we explored the impact of CCH on the expression of cathepsin B and its association with NLRP3 inflammasome and caspase-1 activation. We found that CCH induces upregulation of cathepsin B, which in turn contributes to the activation of NLRP3 inflammasomes and Caspase-1. This cascade of events leads to elevated levels of pro-inflammatory cytokines such as IL-1 $\beta$ , IL-18, and IL-6 in the hippocampus and frontal cortex regions of rat brains.

The experimental rat model employed in this study involved establishing the PBOCCA model. This model was created by permanently ligating both common

carotid arteries, leading to a notable reduction in CBF. Consequently, the rats exhibited deficits in learning and memory and neuronal damage that resembled the conditions observed in patients with VaD. Over time, the PBOCCA rat model has proven to be a valuable tool

for investigating the underlying mechanisms of chronic cerebrovascular disorders and for screening potential therapeutic agents aimed at treating AD and VaD ([Farkas et al., 2007](#); [Kumaran et al., 2021](#); [Kumaran et al., 2022](#); [Shang et al., 2016](#); [Shang et al., 2019](#)).

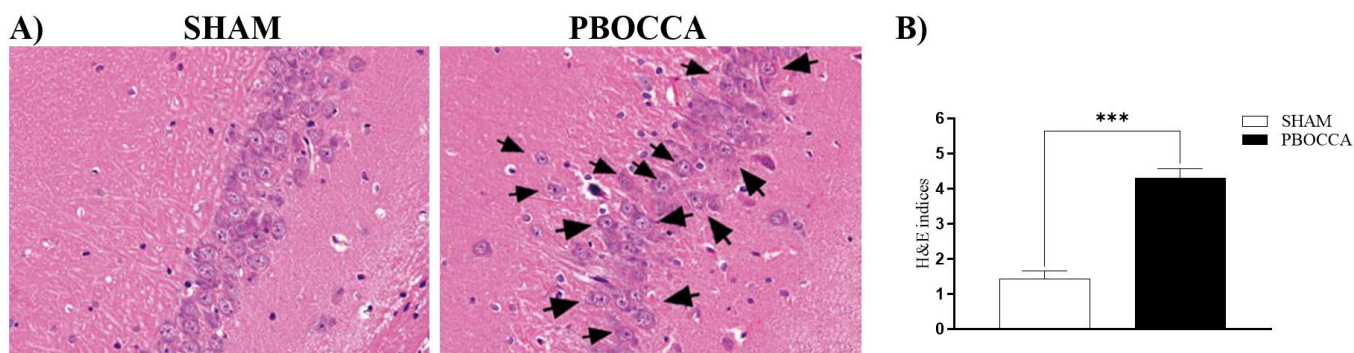


**Figure 3.** Neuronal damage in hippocampal CA1 subfield of PBOCCA rats. **(A)** Representative HE-stained sections showing changes (number of pyknotic neurons) in hippocampal morphology. **(B)** HE staining indices for hippocampal neuronal damage (n = 8 rats/group, \*p < 0.05 Sham vs. PBOCCA).

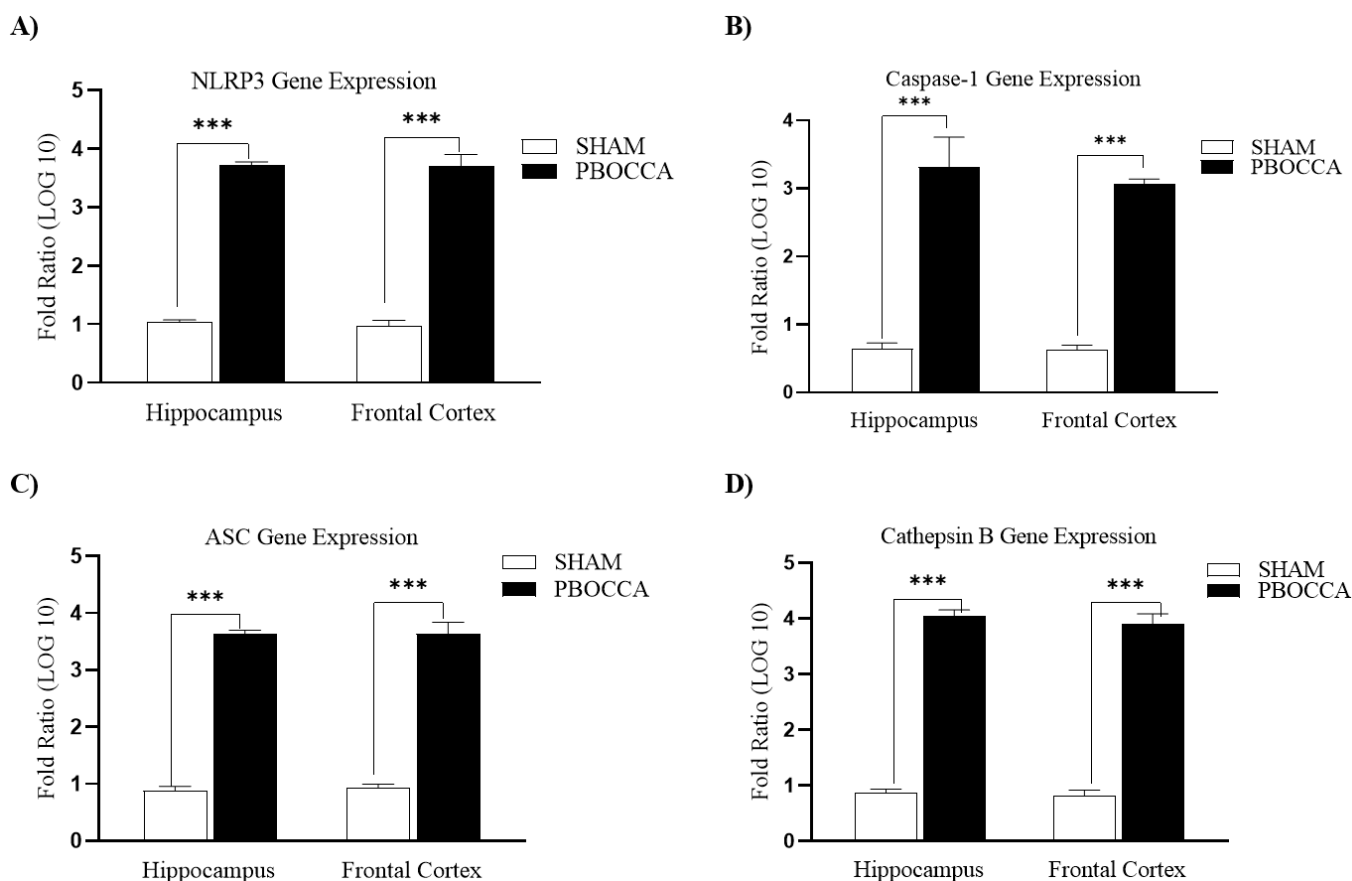


**Figure 4.** The gene expression of NLRP3, Caspase-1, ASC and cathepsin B. **(A-D)** Gene expression histograms for NLRP3, Caspase-1, ASC and cathepsin B in hippocampus and frontal cortex regions. (n = 8 rats/group, \*p < 0.05 Sham vs. PBOCCA).

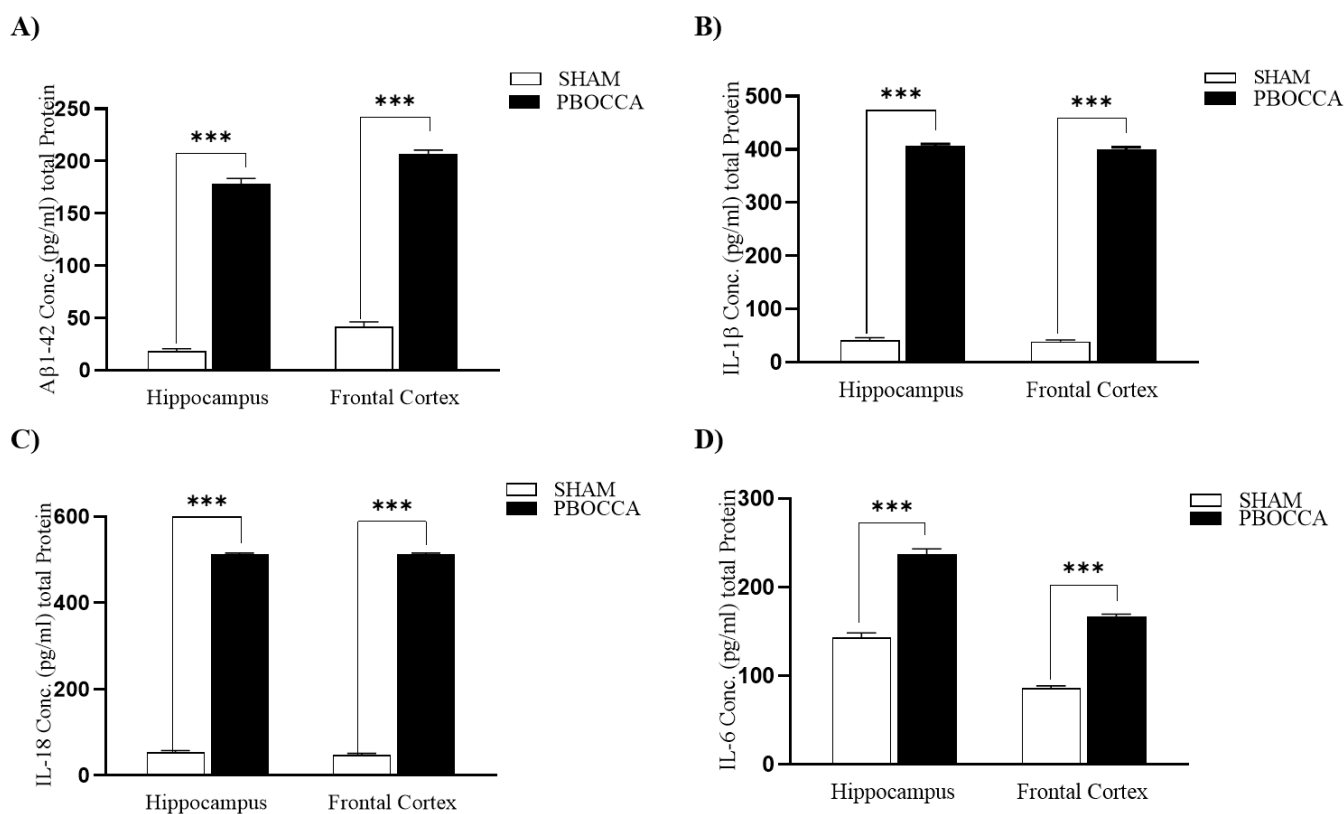


**Figure 5.** The expression of Aβ1-42, IL-1β, IL-18 and IL-6. (A-D) Expression histograms for Aβ1-42, IL-1β, IL-18 and IL-6 in hippocampus and frontal cortex regions. (n = 8 rats/group, \*p < 0.05 Sham vs. PBOCCA).

A series of behavioural tests (open-field test and MWM) were conducted (Kumaran et al., 2022; Wang et al., 2019) in Sham (without ligation) and PBOCCA-operated rats, respectively, to assess both motoric and cognitive functions. Recent studies by Damodaran, Farkas, Kumaran and their colleagues indicated that the CCH model did not exert any apparent effects on basic motor abilities (Damodaran et al., 2020; Farkas et al., 2007; Kumaran et al., 2021, 2022, 2023). In this study, the locomotor activities at day 15 demonstrated a similar effect in PBOCCA rats compared to a Sham control group.

MWM is one of the methods used to assess cognitive impairment in mammals caused by CCH (Bhuvanendran et al., 2019; Cechetti et al., 2012; Deiana et al., 2011; Hazalin et al., 2020). Recent studies demonstrated that learning and spatial memory see a reduction after CCH is induced in PBOCCA rats, as compared to Sham control groups (Hazalin et al., 2020; Tiang et al., 2020). The current study noted significant cognitive impairment in the spatial memory test using the MWM. PBOCCA rats showed a significant increase in escape latencies during the 4-day training session and reduced the percentage of time spent in the target quadrant during the probe trial compared to Sham rats. These findings indicate

that rats exposed to prolonged cerebral ischemia i.e. 2 weeks after PBOCCA surgery, display significant impairments in spatial reference learning and memory, findings that align with previous studies (Damodaran et al., 2014; Kumaran et al., 2021; Tiang et al., 2020).

Rats in both groups demonstrated similar mean swimming speeds during probe trial tests. This indicates that the results obtained from the spatial training and reference memory during probe trials were not affected by any motor dysfunction during swimming, lack of motivation, or vision impairment in PBOCCA rats. These outcomes align with previous studies on the subject (Ahad et al., 2020; Kumaran et al., 2021).

Consistent with previous reports, CCH induced spatial learning and memory deficits with structural damage to the hippocampus in PBOCCA rats (Wang et al., 2017; Wang et al., 2018). In the present study, the H&E-stained brain tissue from CCH-induced rats revealed arrangements of disrupted cellular activity in hippocampal CA1 and significantly increased numbers of pyknotic neurons with cytoplasmic shrinkage. These results are consistent with earlier reports by Wang and colleagues (2019).



Su and colleagues carried out a sequence of investigations, revealing that CCH triggered the release of proinflammatory cytokines, disrupted lysosome function, and led to the accumulation of autolysosomes, ultimately leading to atypical autophagy responses (Su et al., 2018). Nonetheless, the precise underlying mechanisms remain partially elucidated. Recently, the significance of autophagy in modulating the NLRP3 inflammasome within inflammatory conditions of the nervous system has been highlighted (Zhao et al., 2021). Autophagy assumes a counteractive role in controlling the initiation of the NLRP3 inflammasome through the removal of intrinsic inflammasome activators, encompassing ROS originating from impaired mitochondria, inflammatory constituents and cytokines (Biasizzo & Kopitar-Jerala, 2020; Cao et al., 2019). Previous research indicates that abnormal autophagy led to lysosomal membrane destabilisation, K<sup>+</sup> efflux, and release of cathepsin B into the cytosol, which over-activated the NLRP3 inflammasome and increased the IL-1 $\beta$  constituent in primary mouse microglia and BV-2 cells (Wu et al., 2021). A study by Matsuyama and colleagues also revealed that the levels of NLRP3, caspase-1 and IL-1 $\beta$  increased significantly after CCH in the thalamus and hippocampus of AD mice (Matsuyama et al., 2020).

Nevertheless, the impact of autophagy on the NLRP3 inflammasome within the context of CCH remains unexplored. Gene expression was evaluated using RT-PCR to ascertain the potential involvement of autophagy in the stimulation of the NLRP3 inflammasome and to elucidate its potential underlying mechanism in the context of CCH. The results demonstrated that the cathepsin B gene expression level increased after CCH was induced in PBOCCA rats. This enhancement in cathepsin B level has been significantly seen in both hippocampus and frontal cortex after PBOCCA surgery. The present results demonstrated that CCH significantly increased the NLRP3, ASC and caspase-1 gene expressions in PBOCCA rats, which subsequently caused an increment in the level of NLRP3 inflammasome. The findings of RT-PCR analysis illustrated that the level of NLRP3, ASC and caspase-1 gene expressions increased after CCH was induced in PBOCCA rats. This enhancement has been seen significantly after PBOCCA surgery in both hippocampus and frontal cortex. The causal roles that CCH plays in the neuro-pathologies and cognitive impairment characteristic of AD and VaD have been revealed in different studies (Wang et al., 2019; Zhang et al., 2020).

Previous studies revealed that activation of microglia in CCH-induced rats is associated with the release of inflammatory cytokines such as IL-18, IL-1 $\beta$ , and IL-6 which leads to the progression of BBB disruption in AD and VaD patients (Lee et al., 2016; Nath et al., 2020). The present study's ELISA results demonstrated that the amount of IL-1 $\beta$ , IL-18, and IL-6 increased significantly following NLRP3 activation in the PBOCCA control group compared to the Sham group. Findings from prior research have also suggested that the NLRP3 inflammasome undergoes oligomerisation and subsequent activation, leading to the initiation of caspase-1 activation. This activation, in turn, facilitates the processing and subsequent release of IL-1 $\beta$  (Matsuyama et al., 2020) and IL-18 (Roy et al., 2023).

Also, CCH could reduce CBF, as seen in the PBOCCA model (Kumaran et al., 2021; Kumaran et al., 2022). In a prior study, Kitaguchi and colleagues observed that prolonged cerebral hypoperfusion led to heightened A $\beta$  accumulation and facilitated the development of AD pathology (Kitaguchi et al., 2009). The absence of the NLRP3 inflammasome prompted microglial cells to adopt an M2 phenotype, resulting in reduced A $\beta$  deposition (Heneka et al., 2012). We present the first demonstration of how the amount of A $\beta$ <sub>1-42</sub> significantly increased in the PBOCCA group compared to the control group. Therefore, over-amplifying amplification of these immune responses and prolonged reduction of CBF leads to the overproduction of A $\beta$  and a decrease of A $\beta$  uptake by CBF.

On the other hand, insufficient CBF due to PBOCCA surgery reduced A $\beta$  removal by blood vessels, leading to the accumulation of A $\beta$  and activating the innate immune response and NLRP3 inflammasome (Lučiūnaitė et al., 2020). The limitation of this study is that cerebral blood flow should be measured using a laser Doppler flowmetry technology to confirm the reduction of CBF in this animal model. Secondly, other biomarkers must be further investigated to ascertain whether the induction of PBOCCA-induced CCH can be represented as AD, such as hyperphosphorylation of tau protein.

The results of this investigation imply that increased NLRP3 inflammasome expression plays a role in shaping the pathophysiology of individuals affected by vascular cognitive impairment. In brief, the release of proinflammatory cytokines in response to CCH is intricately linked to cognitive decline, particularly in AD progression (Farkas et al., 2007; Rajeev et al., 2022). CCH triggers the activation of NLRP3 inflammasomes in

microglia, leading to the secretion of cytokines such as IL-1 $\beta$ , IL-18 (Shang et al., 2019), and IL-6. These cytokines contribute to neuroinflammation and synaptic dysfunction, exacerbating cognitive impairment observed in AD (Hanslik & Ulland, 2020).

The activation of NLRP3 inflammasomes exacerbates tau pathology and contributes to the spread of A $\beta$  plaques in the brain (Van Zeller et al., 2021). Notably, research demonstrates that NLRP3 inflammasome activation precedes AD pathology, suggesting its involvement as an early pathogenic event in the disease. Our study provides novel insights by elucidating the association between CCH, autophagy, and NLRP3 inflammasome activation. Our study specifically illustrates that CCH leads to an increase in cathepsin B expression, which in turn contributes to the activation of the NLRP3 inflammasome. This activation results in elevated levels of proinflammatory cytokines, including IL-1 $\beta$ , IL-18, IL-6, and A $\beta$ 1-42. These findings underscore a potential mechanistic connection between vascular dysfunction, neuroinflammation, and the progression of AD. These findings underscore the importance of targeting the NLRP3 inflammasome as a therapeutic strategy to mitigate neuroinflammatory processes, inhibit A $\beta$  deposition, and potentially alleviate cognitive decline in AD patients.

## REFERENCES

- Abaricia, J. O., Farzad, N., Heath, T. J., Simmons, J., Morandini, L., & Olivares-Navarrete, R. (2021). Control of innate immune response by biomaterial surface topography, energy, and stiffness. *Acta Biomaterialia*, 133, 58–73. <https://doi.org/10.1016/j.actbio.2021.04.021>
- Ahad, M. A., Chear, N. J., Keat, L. G., Has, A. T. C., Murugaiyah, V., & Hassan, Z. (2023). Bio-enhanced fraction from Clitoria ternatea root extract ameliorates cognitive functions and in vivo hippocampal neuroplasticity in chronic cerebral hypoperfusion rat model. *Ageing Research Reviews*, 89, 101990. <https://doi.org/10.1016/j.arr.2023.101990>
- Ahad, M. A., Kumaran, K. R., Tiang, N., Mansor, N. I., Effendy, M. A., Damodaran, T., Lingam, K., Wahab, H. A., Nordin, N., Liao, P., Müller, C. P., & Hassan, Z. (2020). Insights into the neuropathology of cerebral ischemia and its mechanisms. *Reviews in the Neurosciences*, 31(5), 521–538. <https://doi.org/10.1515/revneuro-2019-0099>
- Bhuvanendran, S., Bakar, S. N. S., Kumari, Y., Othman, I., Shaikh, M. F., & Hassan, Z. (2019). Embelin improves the spatial memory and hippocampal long-term potentiation in a rat model of chronic cerebral hypoperfusion. *Scientific Reports*, 9, 14507. <https://doi.org/10.1038/s41598-019-50954-y>
- Biasizzo, M., & Kopitar-Jerala, N. (2020). Interplay between NLRP3 inflammasome and autophagy. *Frontiers in Immunology*, 11, 591803. <https://doi.org/10.3389/fimmu.2020.591803>
- Calabrese, E. J., Giordano, J., Kozumbo, W. J., Leak, R. K., & Bhatia, T. N. (2018). Hormesis mediates dose-sensitive shifts in macrophage activation patterns. *Pharmacological Research*, 137, 236–249. <https://doi.org/10.1016/j.phrs.2018.10.010>
- Cao, Z., Wang, Y., Long, Z., & He, G. (2019). Interaction between autophagy and the NLRP3 inflammasome. *Acta Biochimica Et Biophysica Sinica*, 51(11), 1087–1095. <https://doi.org/10.1093/abbs/gmz098>
- Cechetti, F., De Souza Pagnussat, A., Worm, P. V., Elsner, V. R., Ben, J., Da Costa, M. S., Mestriner, R. G., Weis, S. N., & Netto, C. A. (2012). Chronic brain hypoperfusion causes early glial activation and neuronal death, and subsequent long-term memory impairment. *Brain Research Bulletin*, 87(1), 109–116. <https://doi.org/10.1016/j.brainresbull.2011.10.006>
- Chen, D., Xu, F., & Zhu, Z. (2022). Progress in the correlation of postoperative cognitive dysfunction and Alzheimer's disease and the potential therapeutic drug exploration. *Ibrain*, 9(4), 446–462. <https://doi.org/10.1002/ibra.12040>
- Cheon, S. Y., Kim, J., Kim, S. Y., Kim, E. J., & Koo, B. (2020). Inflammasome and cognitive symptoms in human diseases: biological evidence from experimental research. *International Journal of Molecular Sciences*, 21(3), 1103. <https://doi.org/10.3390/ijms21031103>

## 5.0 CONCLUSION

In conclusion, the current investigation exhibited that CCH significantly augmented key AD pathologies, encompassing activation of the NLRP3 inflammasome, heightened levels of inflammatory cytokines and A $\beta$ 1-42, and cognitive decline. Therefore, the outcome of this study provided scientific evidence to support the molecular changes in the pathogenesis of AD. Since activation of the NLRP3 inflammasome plays a key role in the pathogenesis of AD, and CCH-induce in PBOCCA rats leads to NLRP3 inflammasome activation through such a molecular and pathological impairment observed in AD, we postulate that CCH via PBOCCA surgery may use as a scientific model for further research.

### Acknowledgements:

The authors received no specific funding, and this work was supported by shared funds from the researchers.

### Author Contributions:

ZA performed the experiments, analysed the data, and wrote the paper; HB, ZH and LNIM contributed research materials and reviewed the manuscript. HK and RBMA reviewed the manuscript.

### Conflicts of Interest:

The authors declared no conflict of interest.

- Damodaran, T., Cheah, P., Murugaiyah, V., & Hassan, Z. (2020). The nootropic and anticholinesterase activities of *Clitoria ternatea* Linn. root extract: Potential treatment for cognitive decline. *Neurochemistry International*, *139*, 104785. <https://doi.org/10.1016/j.neuint.2020.104785>
- Damodaran, T., Hassan, Z., Navaratnam, V., Mustapha, M., Ng, G., Müller, C. P., Liao, P., & Dringenberg, H. C. (2014). Time course of motor and cognitive functions after chronic cerebral ischemia in rats. *Behavioural Brain Research*, *275*, 252–258. <https://doi.org/10.1016/j.bbr.2014.09.014>
- Deiana, S., Platt, B., & Riedel, G. (2011). The cholinergic system and spatial learning. *Behavioural Brain Research*, *221*(2), 389–411. <https://doi.org/10.1016/j.bbr.2010.11.036>
- Farkas, E., Luiten, P., & Bari, F. (2007). Permanent, bilateral common carotid artery occlusion in the rat: A model for chronic cerebral hypoperfusion-related neurodegenerative diseases. *Brain Research Reviews*, *54*(1), 162–180. <https://doi.org/10.1016/j.brainresrev.2007.01.003>
- Hanslik, K. L., & Ulland, T. K. (2020). The role of microglia and the NLRP3 inflammasome in Alzheimer's disease. *Frontiers in Neurology*, *11*, 570711. <https://doi.org/10.3389/fneur.2020.570711>
- Hardy, J., & Selkoe, D. J. (2002). The amyloid hypothesis of Alzheimer's disease: progress and problems on the road to therapeutics. *Science*, *297*(5580), 353–356. <https://doi.org/10.1126/science.1072994>
- Hazalin, N. A. M. N., Liao, P., & Hassan, Z. (2020). TRPM4 inhibition improves spatial memory impairment and hippocampal long-term potentiation deficit in chronic cerebral hypoperfused rats. *Behavioural Brain Research*, *393*, 112781. <https://doi.org/10.1016/j.bbr.2020.112781>
- Heneka, M. T., Kummer, M. P., Stutz, A., Delekate, A., Schwartz, S., Vieira-Saecker, A., Griep, A., Axt, D., Remus, A., Tzeng, T., Gelpí, E., Halle, A., Körte, M., Latz, E., & Golenbock, D. T. (2012). NLRP3 is activated in Alzheimer's disease and contributes to pathology in APP/PS1 mice. *Nature*, *493*(7434), 674–678. <https://doi.org/10.1038/nature11729>
- Kitaguchi, H., Tomimoto, H., Ihara, M., Shibata, M., Uemura, K., Kalaria, R., Kihara, T., Asada-Utsugi, M., Kinoshita, A., & Takahashi, R. (2009). Chronic cerebral hypoperfusion accelerates amyloid  $\beta$  deposition in APPSwInd transgenic mice. *Brain Research*, *1294*, 202–210. <https://doi.org/10.1016/j.brainres.2009.07.078>
- Kumaran, K. R., Wahab, H. A., & Hassan, Z. (2021). In vitro anti-cholinesterase activity and in vivo screening of *Coccoloba uvifera*, *Mimusops elengi* and *Syzygium aqueum* extracts on learning and memory function of chronic cerebral hypoperfusion rat. *Neuroscience Research Notes*, *4*(2), 1–13. <https://doi.org/10.31117/neuroscirn.v4i2.71>
- Kumaran, K. R., Wahab, H. A., & Hassan, Z. (2022). Nootropic effect of *Syzygium polyanthum* (Wight) Walp leaf extract in chronic cerebral hypoperfusion rat model via cholinergic restoration: a potential therapeutic agent for dementia. *Advances in Traditional Medicine*, *23*(3), 833–850. <https://doi.org/10.1007/s13596-022-00653-3>
- Kumaran, K. R., Yunusa, S., Perimal, E. K., Wahab, H. A., Müller, C. P., & Hassan, Z. (2023). Insights into the pathophysiology of Alzheimer's disease and potential therapeutic targets: A current perspective. *Journal of Alzheimer's Disease*, *91*(2), 507–530. <https://doi.org/10.3233/jad-220666>
- Lee, C. H., Park, J. H., Ahn, J. H., & Won, M. (2016). Effects of melatonin on cognitive impairment and hippocampal neuronal damage in a rat model of chronic cerebral hypoperfusion. *Experimental and Therapeutic Medicine*, *11*(6), 2240–2246. <https://doi.org/10.3892/etm.2016.3216>
- Lee, J. M., Lee, J. H., Song, M. K., & Kim, Y. J. (2021). NXP031 improves cognitive impairment in a chronic cerebral hypoperfusion-induced vascular dementia rat model through Nrf2 signaling. *International Journal of Molecular Sciences*, *22*(12), 6285. <https://doi.org/10.3390/ijms22126285>
- Li, D., Fan, H., Yang, R., Li, Y., Zhang, F., & Shi, J. (2022). *Dendrobium nobile* lindl. alkaloid suppresses NLRP3-mediated pyroptosis to alleviate LPS-induced neurotoxicity. *Frontiers in Pharmacology*, *13*, 846541. <https://doi.org/10.3389/fphar.2022.846541>
- Lin, H., Zhang, J., Dai, Y., Liu, H., He, X., Chen, L., Tao, J., Li, C., & Li, W. (2023). Neurogranin as an important regulator in swimming training to improve the spatial memory dysfunction of mice with chronic cerebral hypoperfusion. *Journal of Sport and Health Science*, *12*(1), 116–129. <https://doi.org/10.1016/j.jshs.2022.01.008>
- Lučićnaitė, A., McManus, R. M., Jankunec, M., Rácz, I., Dansokho, C., Dalgėdienė, I., Schwartz, S., Brosseron, F., & Heneka, M. T. (2020). Soluble A $\beta$  oligomers and protofibrils induce NLRP3 inflammasome activation in microglia. *Journal of Neurochemistry*, *155*(6), 650–661. <https://doi.org/10.1111/jnc.14945>
- Mathys, H., Dávila-Velderrain, J., Peng, Z., Gao, F., Mohammadi, S., Young, J. Z., Menon, M., He, L., Abdurrob, F., Jiang, X., Martorell, A. J., Ransohoff, R. M., Hafner, B. P., Bennett, D. A., Kellis, M., & Tsai, L. (2019a). Single-cell transcriptomic analysis of Alzheimer's disease. *Nature*, *570*(7761), 332–337. <https://doi.org/10.1038/s41586-019-1195-2>
- Mathys, H., Dávila-Velderrain, J., Peng, Z., Gao, F., Mohammadi, S., Young, J. Z., Menon, M., He, L., Abdurrob, F., Jiang, X., Martorell, A. J., Ransohoff, R. M., Hafner, B. P., Bennett, D. A., Kellis, M., & Tsai, L. (2019b). Author correction: Single-cell transcriptomic analysis of Alzheimer's disease. *Nature*, *571*(7763), E1. <https://doi.org/10.1038/s41586-019-1329-6>
- Matsuyama, H., Shindo, A., Shimada, T., Yata, K., Wakita, H., Takahashi, R., & Tomimoto, H. (2020). Chronic cerebral hypoperfusion activates AIM2 and NLRP3 inflammasome. *Brain Research*, *1736*, 146779. <https://doi.org/10.1016/j.brainres.2020.146779>

- Nath, D., Khanam, N., & Ghosh, A. (2020). Role of phytochemicals en route blood-brain barrier in cerebral ischemia. *European Journal of Medicinal Plants*, 31(20), 104–115. <https://doi.org/10.9734/ejmp/2020/v31i2030370>
- Pappas, B. A., De La Torre, J. C., Davidson, C., Keyes, M. T., & Fortin, T. (1996). Chronic reduction of cerebral blood flow in the adult rat: late-emerging CA1 cell loss and memory dysfunction. *Brain Research*, 708(1–2), 50–58. [https://doi.org/10.1016/0006-8993\(95\)01267-2](https://doi.org/10.1016/0006-8993(95)01267-2)
- Park, J., Hong, J. H., Lee, S., Ji, H. D., Jung, J., Yoon, K., Lee, J., Won, K. S., Song, B. S., & Kim, H. W. (2019). The effect of chronic cerebral hypoperfusion on the pathology of Alzheimer's disease: A positron emission tomography study in rats. *Scientific Reports*, 9(1), 14102. <https://doi.org/10.1038/s41598-019-50681-4>
- Poh, L., Sim, W. L., Jo, D., Dinh, Q. N., Drummond, G. R., Sobey, C. G., Chen, C., Lai, M. K., Fann, D. Y., & Arumugam, T. V. (2022). The role of inflammasomes in vascular cognitive impairment. *Molecular Neurodegeneration*, 17(1), 1–28. <https://doi.org/10.1186/s13024-021-00506-8>
- Rajeev, V., Fann, D. Y., Dinh, Q. N., Kim, H. A., De Silva, T. M., Lai, M. K., Chen, C., Drummond, G. R., Sobey, C. G., & Arumugam, T. V. (2022). Pathophysiology of blood brain barrier dysfunction during chronic cerebral hypoperfusion in vascular cognitive impairment. *Theranostics*, 12(4), 1639–1658. <https://doi.org/10.7150/thno.68304>
- Roy, J., Wong, K. Y., Aquili, L., Uddin, M. S., Heng, B. C., Tipoe, G. L., Fung, M. L., & Lim, L. W. (2022). Role of melatonin in Alzheimer's disease: From preclinical studies to novel melatonin-based therapies. *Frontiers in Neuroendocrinology*, 65, 100986. <https://doi.org/10.1016/j.yfrne.2022.100986>
- Roy, S., Ansari, M. A., Choudhary, K., & Singh, S. (2023). NLRP3 inflammasome in depression: A review. *International Immunopharmacology*, 117, 109916. <https://doi.org/10.1016/j.intimp.2023.109916>
- Scheffer, S., Hermkens, D., Van Der Weerd, L., De Vries, H. E., & Daemen, M. J. (2021). Vascular hypothesis of Alzheimer disease. *Arteriosclerosis, Thrombosis, and Vascular Biology*, 41(4), 1265–1283. <https://doi.org/10.1161/atvbaha.120.311911>
- Shang, J., Yamashita, T., Zhai, Y., Nakano, Y., Morihara, R., Fukui, Y., Hishikawa, N., Ohta, Y., & Abe, K. (2016). Strong impact of chronic cerebral hypoperfusion on neurovascular unit, cerebrovascular remodeling, and neurovascular trophic coupling in Alzheimer's disease model mouse. *Journal of Alzheimer's Disease*, 52(1), 113–126. <https://doi.org/10.3233/jad-151126>
- Shang, J., Yamashita, T., Zhai, Y., Nakano, Y., Morihara, R., Li, X., Tian, F., Liu, X., Huang, Y., Shi, X., Hishikawa, N., & Ohta, Y. (2019). Acceleration of NLRP3 inflammasome by chronic cerebral hypoperfusion in Alzheimer's disease model mouse. *Neuroscience Research*, 143, 61–70. <https://doi.org/10.1016/j.neures.2018.06.002>
- Simats, A., & Liesz, A. (2022). Systemic inflammation after stroke: implications for post-stroke comorbidities. *EMBO Molecular Medicine*, 14(9), e16269. <https://doi.org/10.15252/emmm.202216269>
- Španić, E., Horvat, L., Ilić, K., Hof, P. R., & Šimić, G. (2022). NLRP1 inflammasome activation in the hippocampal formation in Alzheimer's disease: correlation with neuropathological changes and unbiasedly estimated neuronal loss. *Cells*, 11(14), 2223. <https://doi.org/10.3390/cells11142223>
- Su, S., Wu, Y., Lin, Q., & Hai, J. (2017). Cannabinoid receptor agonist WIN55,212-2 and fatty acid amide hydrolase inhibitor URB597 ameliorate neuroinflammatory responses in chronic cerebral hypoperfusion model by blocking NF-κB pathways. *Naunyn-Schmiedeberg's Archives of Pharmacology*, 390(12), 1189–1200. <https://doi.org/10.1007/s00210-017-1417-9>
- Su, S., Wu, Y., Wei, D., & Hai, J. (2018). Inhibition of excessive autophagy and mitophagy mediates neuroprotective effects of URB597 against chronic cerebral hypoperfusion. *Cell Death and Disease*, 9(7), 733. <https://doi.org/10.1038/s41419-018-0755-y>
- Tiang, N., Ahad, M. A., Murugaiyah, V., & Hassan, Z. (2020). Xanthone-enriched fraction of *Garcinia mangostana* and  $\alpha$ -mangostin improve the spatial learning and memory of chronic cerebral hypoperfusion rats. *Journal of Pharmacy and Pharmacology*, 72(11), 1629–1644. <https://doi.org/10.1111/jphp.13345>
- Van Zeller, M., Dias, D. M., Sebastião, A. M., & Valente, C. A. (2021). NLRP3 Inflammasome: A starring role in Amyloid-B- and TAU-Driven pathological events in Alzheimer's disease. *Journal of Alzheimer's Disease*, 83(3), 939–961. <https://doi.org/10.3233/jad-210268>
- Vorhees, C. V., & Williams, M. T. (2006). Morris water maze: procedures for assessing spatial and related forms of learning and memory. *Nature Protocols*, 1(2), 848–858. <https://doi.org/10.1038/nprot.2006.116>
- Wang, D., Lin, Q., Su, S., Liu, K., Wu, Y., & Hai, J. (2017). URB597 improves cognitive impairment induced by chronic cerebral hypoperfusion by inhibiting mTOR-dependent autophagy. *Neuroscience*, 344, 293–304. <https://doi.org/10.1016/j.neuroscience.2016.12.034>
- Wang, D., Yin, H., Kang, K., Lin, Q., Su, S., & Hai, J. (2018). The potential protective effects of cannabinoid receptor agonist WIN55,212-2 on cognitive dysfunction is associated with the suppression of autophagy and inflammation in an experimental model of vascular dementia. *Psychiatry Research*, 267, 281–288. <https://doi.org/10.1016/j.psychres.2018.06.012>
- Wang, D., Yin, H., Lin, Q., Fang, S., Shen, J., Wu, Y., Su, S., & Hai, J. (2019). Andrographolide enhances hippocampal BDNF signaling and suppresses neuronal apoptosis, astroglial activation, neuroinflammation, and spatial memory deficits in a rat model of chronic cerebral hypoperfusion. *Naunyn-Schmiedeberg's Archives of Pharmacology*, 392(10), 1277–1284. <https://doi.org/10.1007/s00210-019-01672-9>

- Wang, X., Xing, A., Xu, C., Cai, Q., Hong, L., & Liang, L. (2010). Cerebrovascular hypoperfusion induces spatial memory impairment, synaptic changes, and amyloid-B oligomerization in rats. *Journal of Alzheimer's Disease*, 21(3), 813–822. <https://doi.org/10.3233/jad-2010-100216>
- Wu, A., Zhou, X., Qiao, G., Yu, L., Tang, Y., Lu, Y., Qiu, W., Pan, R., Yu, C., Law, B. Y., Qin, D., & Wu, J. (2021). Targeting microglial autophagic degradation in NLRP3 inflammasome-mediated neurodegenerative diseases. *Ageing Research Reviews*, 65, 101202. <https://doi.org/10.1016/j.arr.2020.101202>
- Xu, L., Qu, C., Qu, C., Shen, J., Song, H., Li, Y., Liang, T., Zheng, J., & Zhang, J. (2020). Improvement of autophagy dysfunction as a potential mechanism for environmental enrichment to protect blood-brain barrier in rats with vascular cognitive impairment. *Neuroscience Letters*, 739, 135437. <https://doi.org/10.1016/j.neulet.2020.135437>
- Xu, Y., Yang, Y., Chen, X., Jiang, D., Zhang, F., Guo, Y., Hu, B., Xu, G., Peng, S., Wu, L., & Hu, J. (2023). NLRP3 inflammasome in cognitive impairment and pharmacological properties of its inhibitors. *Translational Neurodegeneration*, 12(1), 49. <https://doi.org/10.1186/s40035-023-00381-x>
- Yu, W., Li, Y., Hu, J., Wu, J., & Huang, Y. (2022). A study on the pathogenesis of vascular cognitive impairment and dementia: The Chronic Cerebral Hypoperfusion hypothesis. *Journal of Clinical Medicine*, 11(16), 4742. <https://doi.org/10.3390/jcm11164742>
- Zhang, J., Sun, P., Zhou, C., Zhang, X., Ma, F., Yang, X., Hamblin, M., & Yin, K. (2020). Regulatory microRNAs and vascular cognitive impairment and dementia. *CNS Neuroscience & Therapeutics*, 26(12), 1207–1218. <https://doi.org/10.1111/cns.13472>
- Zhao, M., Zhang, B., Deng, L., & Zhao, L. (2023). Acrylamide induces neurotoxicity in SH-SY5Y cells via NLRP3-mediated pyroptosis. *Molecular Neurobiology*, 60(2), 596–609. <https://doi.org/10.1007/s12035-022-03098-6>
- Zhao, S., Li, X., Wang, J., & Wang, H. (2021). The role of the effects of autophagy on NLRP3 inflammasome in inflammatory nervous system diseases. *Frontiers in Cell and Developmental Biology*, 9, 657478. <https://doi.org/10.3389/fcell.2021.657478>
- Zhao, Y., Gu, J., Dai, C., Liu, Q., Iqbal, K., Liu, F., & Chen, G. (2014). Chronic cerebral hypoperfusion causes decrease of O-GlcNAcylation, hyperphosphorylation of tau and behavioral deficits in mice. *Frontiers in Aging Neuroscience*, 6, 10. <https://doi.org/10.3389/fnagi.2014.00010>